Effect of Polytetrafluoroethylene (PTFE) and micro porous layer (MPL) on thermal conductivity of fuel cell gas diffusion layers: Modeling and experiments

Hamidreza Sadeghifar [a], Ned Djilali [b], Majid Bahrami [a],[*]

[a] School of Mechatronic Systems Engineering, Simon Fraser University, Surrey V3T 0A3, BC, Canada
[b] Department of Mechanical Engineering and Institute for Integrated Energy Systems, University of Victoria, Victoria V8W 3P6, BC, Canada

HIGHLIGHTS

- An analytic robust model is developed for estimating GDL thermal conductivity.
- The model considers PTFE addition to the GDL.
- Thermal conductivity of MPL is accurately measured in a compression range of 2–14 bar.
- Effect of thermal conductivity on PTFE, MPL, and compression is considered.
- Thermal contact resistances between GDL and MPL/iron surface are measured.

GRAPHICAL ABSTRACT
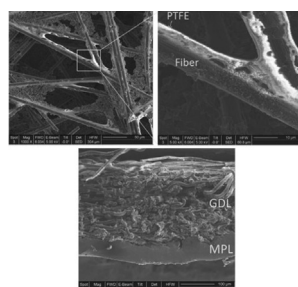
ABSTRACT

Through-plane thermal conductivity of 14 SIGRACET gas diffusion layers (GDLs), including series 24 & 34, as well as 25 & 35, and of micro porous layer (MPL) is accurately measured under different compression, ranging from 2 to 14 bar, at a nominal temperature of 60 °C. The effect of compression, PTFE loading, and of MPL on thermal conductivity and contact resistance is investigated experimentally, and measurements are presented for the first time for the contact resistance between an MPL and a GDL for an MPL-coated GDL substrate. A new and robust mechanistic model is presented for predicting the through-plane thermal conductivity of GDLs treated with PTFE and is successfully verified with the present experimental data. The model predicts the experimentally-observed reduction in thermal conductivity as a result of PTFE treatment, and provides detailed insights on the functional dependence of thermal conductivity on geometric parameters, compression, and PTFE. The model can be used in performance modeling and in design of polymer electrolyte membrane fuel cells.

© 2013 Elsevier B.V. All rights reserved.

1. Introduction

The efficiency and performance of proton exchange membrane fuel cells (PEMFCs) is highly dependent on heat and the associated water transport because of the low operating temperature, which is typically less than 90 °C [1–5]. One of the parameters that directly

* Corresponding author. Tel.: +1 (778) 782 8538; fax: +1 (778) 782 7514.
E-mail addresses: sadeghif@sfu.ca (H. Sadeghifar), ndjilali@uvic.ca (N. Djilali), mbahrami@sfu.ca (M. Bahrami).

affects both heat and water management of a PEMFC, as well as durability and longevity of its components, is the temperature distribution inside the membrane electrode assembly (MEA) [6–11]. This temperature distribution is highly dependent on the thermal conductivity of the components, especially gas diffusion layer (GDL) [12–14]. Hence, accurate prediction of the GDL thermal conductivity and quantifying its dependency on salient parameters such as compression, micro-structural characteristics, additive materials such as Polytetrafluoroethylene (PTFE) and micro porous layer (MPL) are essential for understanding and improving the performance and longevity of PEMFCs.

GDLs are usually treated with varying amounts of hydrophobic PTFE for the purpose of water management. This can change the thermal resistance of a GDL and, consequently, heat management. The few studies performed to date to measure and model the thermal conductivity of GDLs treated with PTFE have produced conflicting trends. Khandelwal and Mench [15] and Burheim et al. [16,17] reported that PTFE treatment leads to a reduction in thermal conductivity whereas Zamel et al. [12] did not observe any changes with PTFE additions as high as 60 wt%. On the other hand, the models developed by Yablecki and Bazylak [18] and Fishman and Bazylak [19] both predict a noticeable increase in thermal conductivity with increasing PTFE content. This paper attempts to resolve some of the issues through a new set of systematic measurements and a mechanistic model that considers salient physical and geometrical features.

The present model results are compared and successfully validated with thermal conductivity measurements of several SIGRA-CET GDLs treated with varying PTFE content. In addition, the effect of an MPL on thermal conductivity and thermal contact resistance of GDLs is investigated experimentally. Moreover, the contact resistance between an MPL and a GDL substrate, which to the authors' knowledge has not been documented to date, is measured for the first time in this paper. The impact of cyclic loading and hysteresis behavior on the GDL thermal resistance is experimentally investigated and presented.

2. Model development

A statistically-based mechanistic model for predicting the through-plane thermal conductivity of untreated GDLs was previously developed by the present authors in Ref. [20]. The untreated GDL model took into account the salient effects of geometrical parameters and operating conditions, and also considered the spreading/constriction resistances between touching fibers [20,21]. This model is extended in this paper to account for PTFE treatment of GDLs.

Examination of microscope images of treated GDL samples, such as the ones shown in Fig. 1, indicates that a considerable portion of PTFE accumulates at the intersection of fibers (Fig. 1b). For convenience, we refer to the portions corresponding to the upper and lower halves in the through-plane directions as PTFE′ and PTFE″ respectively. In addition, some PTFE (PTFE‴) cover each fiber randomly (Fig. 1a and c) and a thin layer of PTFE on the first and last layers of fibers in the GDL (PTFE layer) can be seen (Fig. 1a). A geometric model representation of a PTFE-treated GDL is illustrated in Fig. 2. The model considers the general case of non-homogeneous penetration, which allows representation of PTFE penetrating into all or only some of the layers at each side. The PTFE treatment procedure commonly used in industry, in which the GDL is dipped in a PTFE solution, is consistent with the latter case with penetration confined to the layers in proximity to the surface. It should also be noted that geometric characteristics such as fiber spacing and angle distribution will not change as a result of PTFE treatment.

The present model is based on a unit cell approach that considers a GDL as a periodic fibrous microstructure with a corresponding resistive network through which heat transfer takes place [20,21]. Extending the unit cell defined in Refs. [20,21] for untreated GDLs, a unit cell consisting of two blocks is taken here to represent the fiber layers containing PTFE and a second unit cell represents the first and last fiber layers with a thin coating of PTFE layers on both surfaces of GDLs, as shown in Figs. 2 and 3.

For a GDL treated with PTFE, the thermal resistance network of the entire GDL, depicted in Fig. 4a–c, will be:

$$
\begin{aligned}
R_{\text{tot}} = {} & 2\left(\frac{1}{R_{\text{free air}}} + \frac{1}{R_{\text{PTFE layer}}}\right)^{-1} \\
& + \frac{n_{\text{with PTFE}}}{2}\left[\frac{1}{R_{g,1} + R_{\text{PTFE}'''}} + \frac{1}{R_{gc',1}} + \frac{1}{R_{1,\text{PTFE}''}} + \frac{1}{R_{co}}\right]^{-1} \\
& + \frac{n_{\text{with PTFE}}}{2}\left[\frac{1}{R_{g,2}} + \left(\frac{1}{R_{gc',2}} + \frac{1}{R_{2,\text{PTFE}'}}\right) + \frac{1}{R_{sp}}\right]^{-1} \\
& + \frac{n_{\text{without PTFE}}}{2}\left[\frac{1}{R_{g,1}} + \frac{1}{R_{gc,1}} + \frac{1}{R_{co}}\right]^{-1} \\
& + \frac{n_{\text{without PTFE}}}{2}\left[\frac{1}{R_{g,2}} + \frac{1}{R_{gc,2}} + \frac{1}{R_{sp}}\right]^{-1}
\end{aligned}
$$

$$(1)$$

where all the resistances of R_{co}, R_{sp}, $R_{g,1}$, $R_{g,2}$, $R_{gc,1}$, $R_{gc,2}$, $R_{gc',1}$, and $R_{gc',2}$ are defined as in Refs. [20,21], and $R_{\text{PTFE layer}}$ and $R_{\text{free air}}$ are as follows:

$$
R_{\text{PTFE layer}} = \frac{t_{\text{PTFE}}}{k_{\text{PTFE}}\frac{\pi d(l+w)}{4}} \tag{2}
$$

$$
R_{\text{free air}} = \frac{\frac{d}{2} + t_{\text{PTFE}}}{k_{\text{air}}\frac{(l-d)(w-d)}{4}} \tag{3}
$$

where k_{PTFE} and k_{air} are thermal conductivities of PTFE and air, respectively, and t_{PTFE} is the average thickness of PTFE coating on the fibers of the first and last layers of GDL, given later in Table 1. l, w, and d are the geometrical parameters shown in Fig. 2, which have already been given in Ref. [20] for the studied GDLs.

Note that all PTFE resistances inside the GDL, i.e., $R_{\text{PTFE}'}$, $R_{\text{PTFE}''}$, and $R_{\text{PTFE}'''}$, are in parallel to a much lower resistance, that is, conduction through fiber–fiber contacts, and therefore, will not have a noticeable impact on the total resistance of the GDL, see Eq. (1). Accordingly, these PTFE resistances have secondary effects and need not be considered for estimating the total resistance of the entire GDL. Note also that although the thermal conductivity of PTFE is one order of magnitude higher than that of air ($k_{\text{air}} = 0.026 < k_{\text{PTFE}} = 0.3$ W m^{-1} K^{-1} [3]), it is still some orders of magnitude lower than the thermal conductivity of the fibers. As such, one can conclude that PTFE treatment on GDLs can be modeled as only one "thin layer" on the top/bottom layers of GDLs and will only affect the through-plane thermal conductivity and the thermal contact resistance at the interface of GDL-bipolar plate. For this reason, the PTFE distributed inside the GDL does not have a noticeable impact on the through-plane thermal conductivity (also see Ref. [20]). Hence, from the viewpoint of through-plane heat transfer, the thermal resistance of a PTFE-treated GDL can be practically approximated in terms of untreated GDL, PTFE, and gas (air) resistances as:
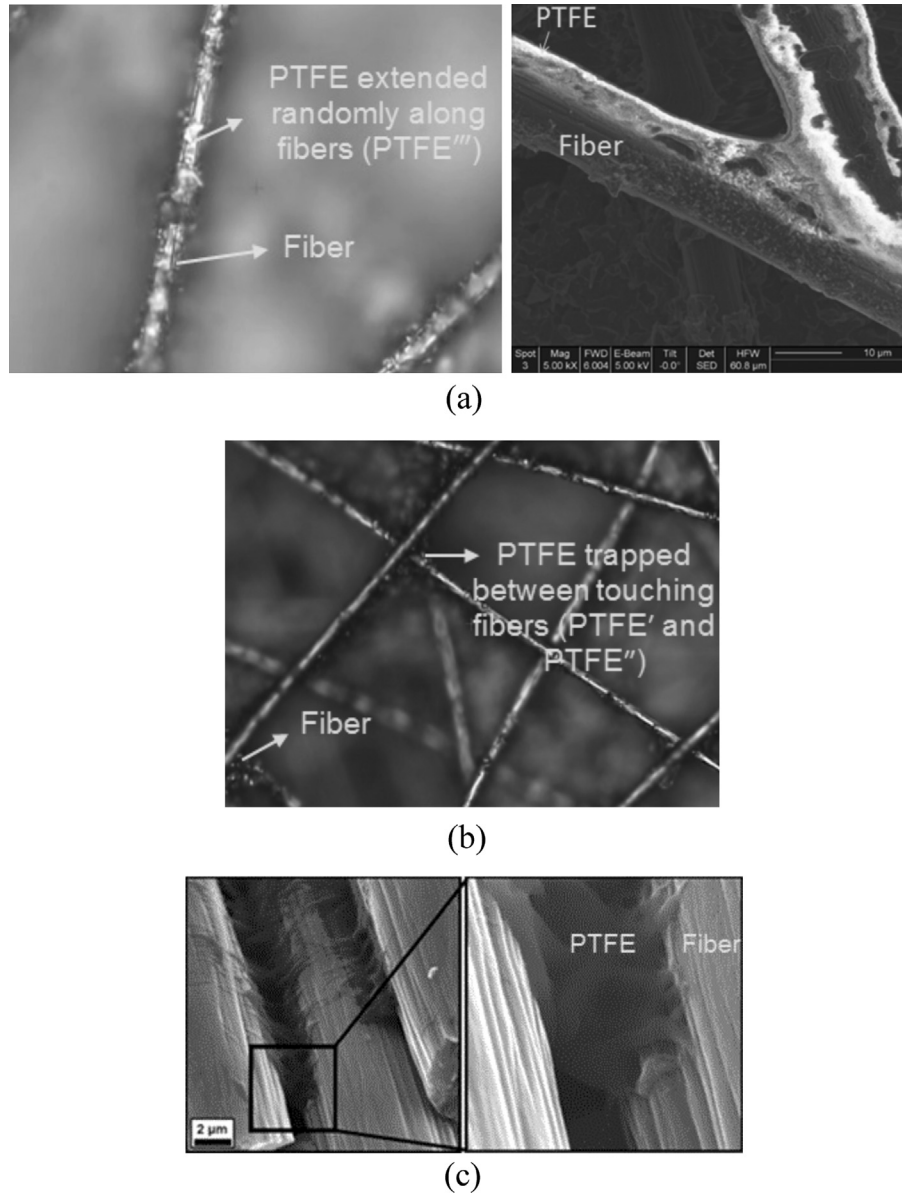
(a)

(b)

(c)

Fig. 1. PTFE distribution inside different GDLs: (a) and (b) SGL 24BA (present study) and (c) ELAT [22].

$$R_{tot}^{PTFE-treated\ GDL} \approx (n-1)R_{tot}^{Untreated\ GDL}$$

$$+ 2\left(\frac{1}{R_{free\ air}} + \frac{1}{R_{PTFE\ layer}}\right)^{-1} \tag{4}$$

where n is the number of fiber layers ($=t_{GDL}/d$).

The thermal conductivity of GDL can finally be calculated by:

$$k_{eff} = \frac{4t_{GDL}}{lwR_{tot}} \tag{5}$$

It should be noted that resin and other additive materials, which can be randomly distributed inside the "carbon fiber *skeleton*" of the GDL, have not been considered at this stage of our work. However, the modeling framework allows for the treatment of such additives in a similar way to PTFE. The fiber–fiber resistance is always much less than other resistances, including fiber–X–fiber resistance where X can be any phenolic resin or filler. It should be noted that fiber–X–fiber resistance includes the bulk resistance of the lower-conductivity material X as well as two contact resistances of X with the adjacent fibers.

3. Experimental study

3.1. GDL samples

Different treated and untreated SIGRACET gas diffusion layers, series SGL 24 and 34, as well as 25 and 35, were tested to obtain their thermal conductivity. The advantage of working with this type of GDLs is that the effect of PTFE and MPL on their thermal resistances can be separately investigated. Substrates of SGL BA and DA are fabricated by adding 5 and 20 wt% PTFE to the *plain* (untreated) substrate AA, respectively, and the BC type is the BA substrate with MPL on one side, see Fig. 5 [24]. The numbers 24 and 34, as well as 25 and 35, included in the GDL names, refer to their thicknesses, as reported in Table 1. Hence, the only difference between the substrates of SGLs 24 and 34 and those of SGLs 25 and 35 is their thicknesses, which makes the two-thickness method
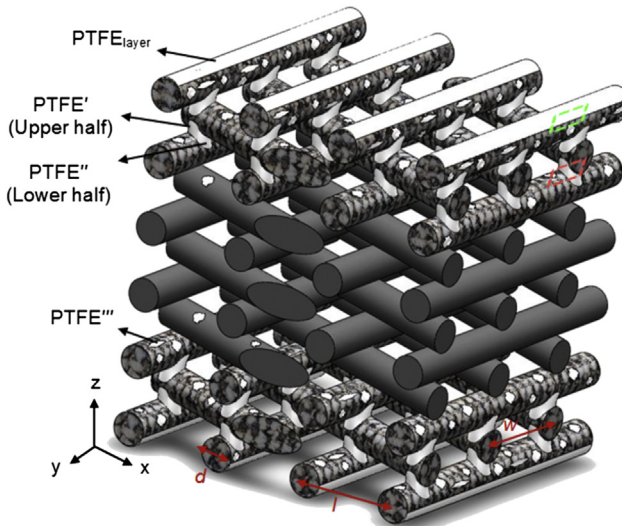
Fig. 2. Geometric model of GDLs treated with PTFE, see Eq. (1).

(a) Resistances of layers without PTFE (middle layers)
(the negligible bulk resistance of fibers has been omitted)

(b) Resistances of layers with PTFE
(the negligible bulk resistance of fibers has been omitted)

[14,20] an appropriate approach for measuring thermal conductivity and contact resistance.

- GDLs with MPL on one side

GDLs coated with MPL on one side, such as SGL BC types, or on both sides [26,27], provide better electrical contacts between the GDL and catalyst or BPP and reduce ohmic losses, as the main component of MPL is the high electrical conductive material of carbon black. However, due to the very low thermal conductivity of carbon black and the hydrophobic agent of PTFE mixed with it, MPL may adversely influence the heat transfer in the fuel cell stack. As a result, knowing the thermal conductivity of MPL, as well as its thermal contact resistance with the GDL substrate, can be useful to the heat management of fuel cells. However, due to the complication associated with maintaining the integrity of this layer after separation from the substrate, experimental measurements of its thermal conductivity can be troublesome [28]. This problem is bypassed in the present study using the procedures described below.
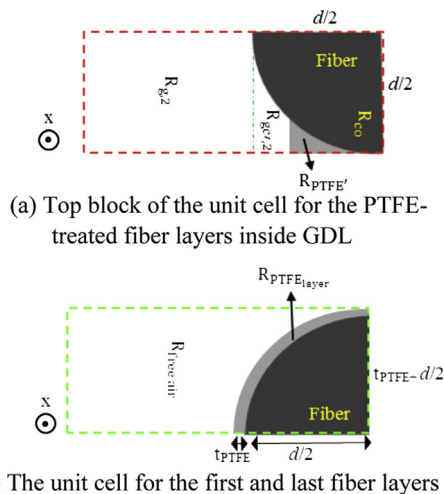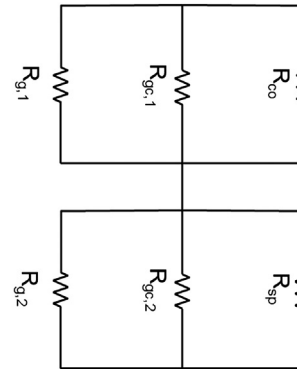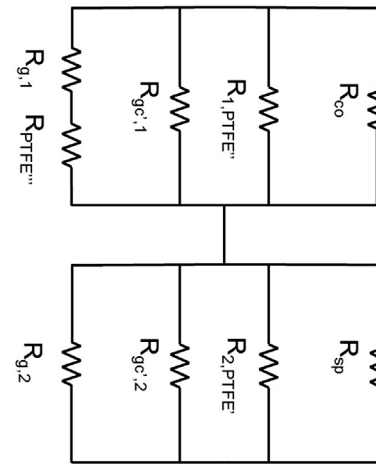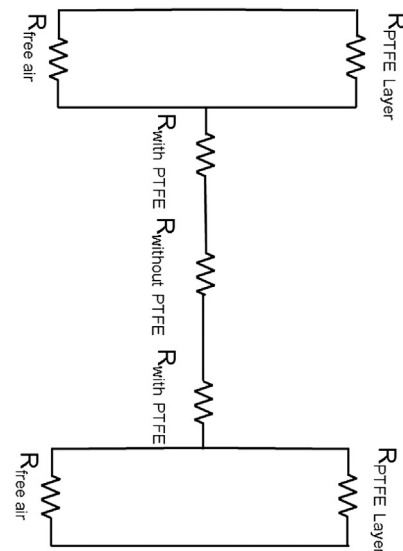

(a) Top block of the unit cell for the PTFE-treated fiber layers inside GDL

(b) The unit cell for the first and last fiber layers

Fig. 3. Unit cells and top block defined for a PTFE-treated GDL.

(c) The total thermal resistance network of the GLD treated with PTFE

Fig. 4. Thermal resistance network for a PTFE-treated GDL.

Table 1
Specifications of SIGRACET GDLs studied in the present work.

SGL	24				25			34				35		
	AA	BA	DA	BC	AA	BA	BC	AA	BA	DA	BC	AA	BA	BC
Porosity (%)	88	84	72	76	92	88	80	88	84	72	76	92	88	80
Thickness (μm) ± 5	190	190	190	235	190	190	235	280	280	280	315	300	300	325
PTFE Thickness on each surface (μm)	0	1.5	3	–	0	1	–	0	1.5	3	–	0	1	0

The total thermal resistance inside a GDL treated with MPL, as shown in Fig. 6, can be written as:

$$R_{GDL} = R_{sub} + R_{MPL} + TCR_{sub-MPL} \qquad (6)$$

It is important to note that although the MPL and GDL substrate interpenetrate rather than form a distinct and well-defined interface, there is nonetheless a contact resistance between the two media, $TCR_{sub-MPL}$, which has been overlooked in all the previous studies aimed at determining the GDL thermal conductivity, see e.g. Refs. [29–31]. This resistance should be deconvoluted from the bulk resistance of the GDL. Having measured the thermal resistance of a GDL coated with MPL, the thermal bulk resistance of the MPL and its thermal contact resistance with the GDL substrate can be obtained using the two-thickness method (see Appendix A). The determination of the MPL conductivity (Eq. (A.2)) is independent of the contact resistance between the substrate and MPL.

3.2. Apparatus and measurement principle

All thermal conductivities measurements are performed using a custom-built thermal contact resistance (TCR) machine, whose design is based on the principle of the guarded heat fluxmeter device recommended by the ASTM Standard C-177. The details of the testbed and the experimental procedure can be found elsewhere [32–35]. The principle utilized in thermal resistance measurements is based on a precise de-convolution of the contact resistance of GDLs with clamping surface from their bulk resistances using the two-thickness method. Detailed explanations on the principle of the thermal contact resistance are given in Refs. [36,37].

3.3. Testbed accuracy

Using two Pyrex 7740 calibration samples with different thicknesses, which have thermal resistances in the same order of magnitude of typical GDLs, the accuracy of the TCR machine was verified. The test results were very satisfactory, as the average

measurement deviation was approximately 5% and the maximum measurement difference observed was 8%.

3.4. Uncertainty analysis

$$\frac{\delta R}{R} \text{ or } \frac{\delta k}{k} = \sqrt{\left(\frac{1}{2}\right)\left(\frac{\delta Q}{Q}\right)^2 + \left(\frac{\delta \Delta T}{\Delta T}\right)^2 + \left(\frac{\delta t}{t}\right)^2 + \left(\frac{\delta A}{A}\right)^2 + \left(\frac{\delta P}{P}\right)^2 + \left(\frac{\delta k_{FM}}{k_{FM}}\right)^2 + \left(\frac{\delta x}{x}\right)^2} \qquad (8)$$

The uncertainty in the total resistance and thermal conductivity measurements of the test apparatus can be calculated in the same manner as [14,15,26,33–35]. The resistance and thermal conductivity are functions of the following parameters:

$$R \text{ or } k = f(Q, \ \Delta T, \ t, \ A, \ P, \ k_{FM}, \ x) \qquad (7)$$

The maximum uncertainty for the thermal resistance and conductivity measurements can be calculated from

All the parameters and the associated uncertainties have been thoroughly defined in related work [25,34] and are summarized in Table 2. Note that the main uncertainty stems from the heat flow rate passing through the fluxmeters, Q. The maximum uncertainty in this study is ±6.6%.

4. Results and discussion

Using the two-thickness method, the thermal conductivity of various GDLs and their thermal contact resistance with the clamping surface (iron fluxmeters) was obtained as a function of

Fig. 5. GDLs of SGL AA, BA, DA, and BC (the black layer represents MPL).
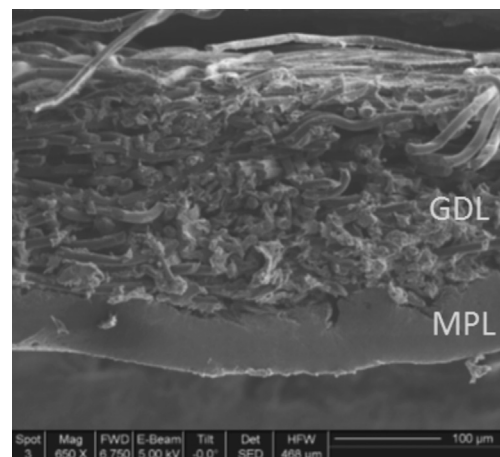
Fig. 6. SEM image of the cross-section of a GDL with an MPL (substrate/MPL assembly of SGL 35 BC).

Table 2
Uncertainty of involving parameters in the thermal resistance measurements in the present study.

$\delta Q/Q$	$\delta \Delta T/\Delta T$	$\delta t/t$	$\delta A/A$	$\delta P/P$	$\delta k_{FM}/k_{FM}$	$\delta x/x$
0.0657	0.0031	0.0005	0.0015	0.05	0.0027	0.01

compression. The effect of PTFE loading (content), MPL, and compression is discussed in the following subsections.
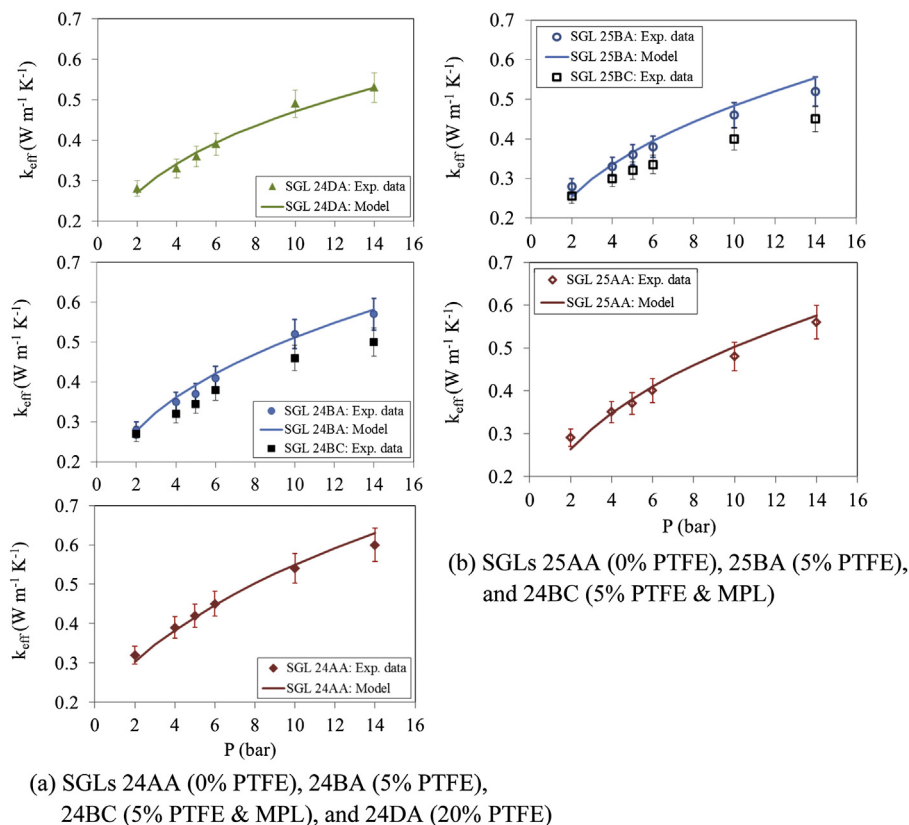
4.1. Effect of PTFE

- Model validation

The thermal conductivities of SGL 24 & 34 AA, BA, DA, and BC and those of series 25 & 35 AA, BA, and BC are shown in Fig. 7. The model predictions are in very good agreement with the experimental data for the PTFE-treated; the most significant feature is that the model captures the experimental trend, i.e., as PTFE content increases the through-plane thermal conductivity decreases. Fig. 7 also depicts the effect of different PTFE loading on the through-plane thermal conductivity. The reduction in thermal conductivity with PTFE is clearly depicted in Fig. 7c and can be attributed to the low thermal conductivity of PTFE, which increases the overall thermal resistance of the entire GDL. The trend observed here is in qualitative agreement with the results of Khandelwal and Mench [15] and Burheim et al. [16,17], but not with the negligible changes reported in Ref. [12] even for 60 wt% PTFE. The present trends are opposite to the model predictions of Yablecki and Bazylak [18] and Fishman and Bazylak [19] which is representative of the distribution of PTFE in the bulk of the GDL but overlooks the

thin coating of PTFE that forms on the surface of the first and last fiber layers. PTFE distributed inside the GDL does not have any noticeable impact on through-plane thermal conductivity. Although PTFE displaces air "pores" that have lower thermal conductivity and reduces the GDL porosity, it does not enhance the overall thermal conductivity of the GDL as noted earlier in the Model development section.

It is interesting to note that the highest decrease observed in thermal conductivity on Fig. 7c pertains to an increase in PTFE from 5 to 20 wt%. The effect of 5% PTFE loading is negligible, as the data of substrates AA (0% PTFE) and BA (5% PTFE) almost overlap or are very close to each other. The general trend of PTFE loading in thermal conductivity reduction is the same for the two series SGL GDLs investigated, and are accurately reproduced by the analytical model.

It is important to note that, unlike the through-plane thermal conductivity, the in-plane one does not decrease with PTFE; rather, a slight increase was observed in Ref. [35]. This is attributed to the very thin layer of PTFE covering the fiber layers on both surfaces of GDL which only influences the GDL thermal resistance in the through-plane direction and has no impact on the in-plane conduction. However, since the low thermal conductivity material of air will be replaced by PTFE, it is reasonable to expect a slight increase in the in-plane thermal conductivity, as observed experimentally and predicted analytically in Ref. [35] (see Fig. 8). However, Zamel et al. [13] reported an opposite trend. This might be due to their use of a simple mixing rule instead of direct measurement to estimate the bulk values of the heat capacity and, eventually, of the thermal conductivity of the GDLs studied in Ref. [13]. In addition, the transient method employed in Ref. [13] for the thermal conductivity measurements is not appropriate for porous materials [14,38].

(a) SGLs 24AA (0% PTFE), 24BA (5% PTFE),
24BC (5% PTFE & MPL), and 24DA (20% PTFE)

(b) SGLs 25AA (0% PTFE), 25BA (5% PTFE),
and 24BC (5% PTFE & MPL)

Fig. 7. Variation of thermal conductivity with pressure: comparison of model predictions with experiments for GDLs with different PTFE loadings and comparison between all the studied GDLs.
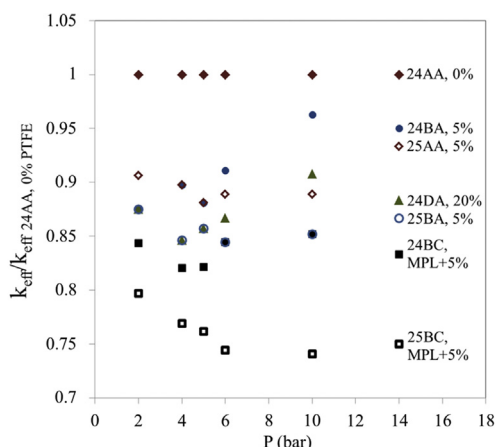
(c) Comparison between thermal conductivities of the studied GDLs with reference to the thermal conductivity of SGL 24AA (0% PTFE)

Fig. 7. (*continued*).

- Thermal contact resistance of PTFE-treated GDLs

The data of the thermal contact resistance between each of GDLs and the iron fluxmeters in Fig. 9 show that PTFE increases the thermal contact resistance. Remarkably, at lower compressive pressures, the thermal contact resistance becomes much more sensitive to PTFE content. In other words, with increasing compression, the effect of PTFE on thermal contact resistance decreases. These results provide qualitative insights into the thermal contact resistance between a metallic bipolar plate [39] and GDL, as function of PTFE loading, compression, porosity, and characteristic fiber spacing.

4.2. Thermal conductivity and effect of MPL

Fig. 10 shows the thermal conductivity of MPLs of SGL 24BC and SGL 25BC, measured in the present study, as a function of compression. The thermal conductivity of both MPL increases with compression up to around 10 bar and then decreases with that. The
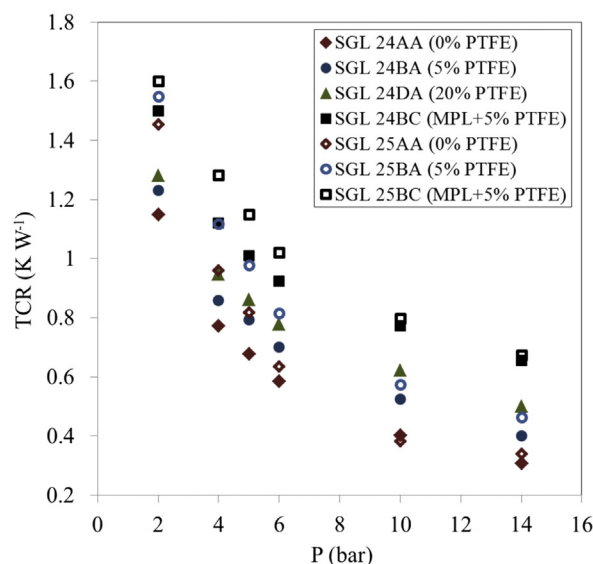

Fig. 9. Thermal contact resistance of different GDLs with iron clamping surfaces as a function of compression: effect of PTFE loading and MPL.

thermal conductivity of SGL 24BC MPL lay in the range of 0.37–0.55, showing a little lower values of thermal conductivity compared to the ones of MPL SGL 25BC ranging from 0.41 to 0.71 W m^{-1} K^{-1} within a compression range of 2–14 bar. Note that the penetration depths and the interfacial contact resistances of the two MPLs coated on SGL 24BC and SGL 25BC are different as their substrates, i.e., SGL 24BA and SGL 25BA, differ from each other in terms of porosity and aspect ratio [20].

It should be noted that the SGL GDLs of type BC are fabricated with an MPL coating on one side of SGL BA with 5 wt% PTFE. In order to accurately determine the effect of MPL on the thermal conductivity of GDLs and their contact resistances with other materials, the results of BC type materials are compared with BA types. Figs. 7 and 9 show that MPL reduces thermal conductivity to some extent and increases contact resistance dramatically. This finding is in qualitative agreement with [14] but not with the result of another study conducted by the same group on the same type of
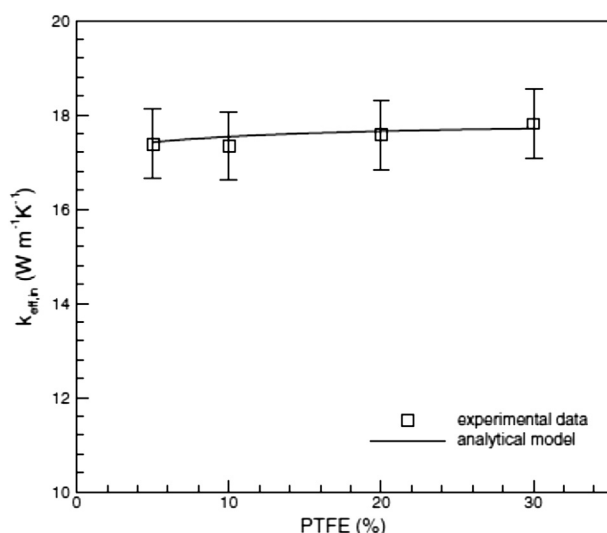

Fig. 8. In-plane thermal conductivity of Toray carbon paper TGP-H-120 over a range of PTFE contents [35].
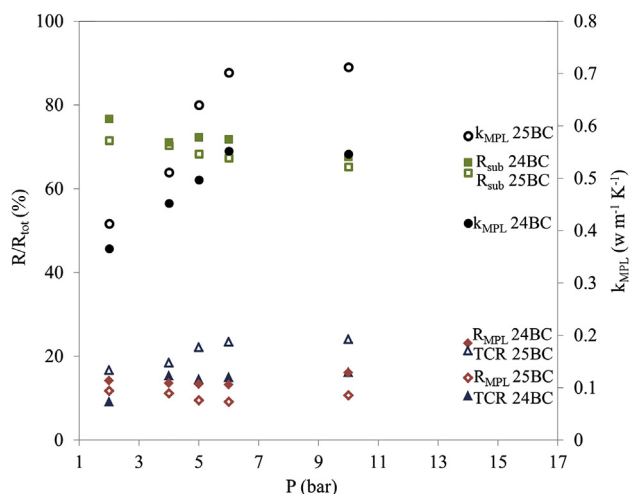

Fig. 10. Thermal conductivity of MPL and contribution of bulk and interfacial resistances inside a GDL−MPL assembly (Eq. (6)): TCR here represents the contribution of the thermal contact resistance between MPL and the GDL substrate to the total resistance.

GDL (SolviCore) [25] reporting a negligible contact resistance of MPL with iron clamping surfaces. This uncorroborated finding of Ref. [25] was attributed to the high surface contact area of the MPL. It should be noted that none of the previously reported measurements of MPL thermal conductivity [14,17,25] accounts for the TCR between MPL and substrate. In addition, the tests of [14,25,33] were not performed in a vacuum chamber and the thermal contact resistance between stacked GDLs was simply omitted.

- Thermal resistances inside GDLs containing MPL

Fig. 10 also presents the contribution of each resistance in Eq. (6) to the total resistance of the GDLs SGL 24BC and 25BC, and reveals that the thermal contact resistance between substrate and MPL is in fact comparable with the resistance of the MPL itself. It should be noted that the thickness of substrate in SGL BC is several times (~7 times) higher than that of the MPL. Assuming the same thickness of MPL and substrate, it could be argued that the thermal contact resistance between substrate and MPL, which is independent of the thickness of either component, can exceed either of the substrate and MPL resistances.

Fig. 10 also shows that with increasing compression pressure (up to 10 bar), the impact of MPL on contact resistance and on the GDL thermal conductivity becomes more pronounced, and in general, the contribution of MPL to the increased total resistance increases. Note that the contribution of MPL resistance to the GDL resistance is proportional to the ratio of the MPL thickness to the substrate one. For GDL substrates with thermal conductivities sufficiently higher than that of the MPL, this ratio should be kept as low as possible in order to reduce the adverse influence of MPL on the bulk thermal conductivity of the GDL.

4.3. Effect of compression

The thermal conductivity of all the GDLs increases with compression as shown in Figs. 7 and 9, whereas their thermal contact resistance with the clamping surface decreases. These reductions in the bulk and contact resistances can be attributed to a better contact between fibers of two adjacent layers and between the GDL and the iron clamping surface (fluxmeters) under higher compression, respectively.
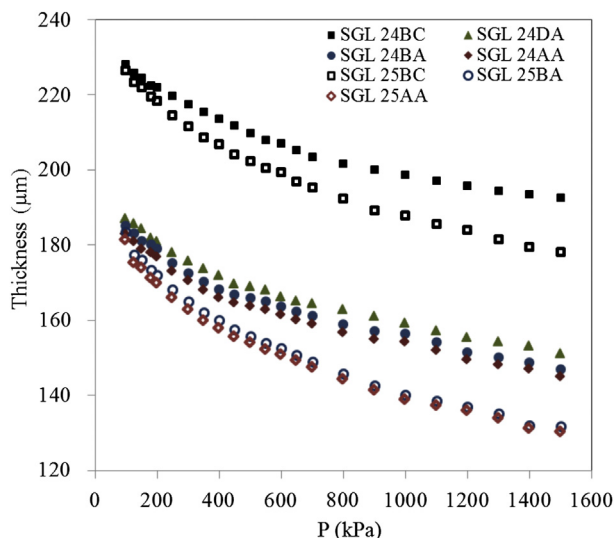
- Thickness variation with compression

Carbon-based gas diffusion layers, typically made of 30–50 layers of carbon fibers attached to each other, are of thicknesses ranging from 150 to 500 μm. Because of the porous nature of the GDL and the elastic nature of the carbon fibers, the thickness of GDLs can change notably with compression. Fig. 11 shows the variations in thickness with pressure increasing up to 15 bar. The curves for each GDL exhibit two parts, a non-linear, almost exponential part extending up to about 7 bar, where the reduction in thickness is steep, and a shallower linear part thereafter for pressure increases from 7 to 15 bar. These trends for the SGL GDLs are consistent with the results in Refs. [14,23,40]. Unsworth et al., on the other hand, reported a linear behavior for entire range of compression for SolviCore GDLs with and without MPL [25].

4.4. Effect of cyclic load

Fuel cell components may experience hundreds of thousands of load cycles during their lifetime [41]. The investigation of load cycling effects is important as they induce internal stresses and deformation and exacerbate a variety of chemical and mechanical degradation mechanisms. Fig. 12 depicts the effect of cyclic loading on the total resistance of SGL 34BC at the temperature of 60 and in the pressure range of 77–820 kPa. As seen, the successive cycling loads practically reduce the total resistance, and this reduction still exists until 8th loading. However, the highest reduction, almost 20%, occurs between the first and second loadings. With increasing the compression pressure, the effect of cyclic loading on the total resistance reduces. The more pronounced difference between loading and unloading of one cycle is evidently observed for the first cycle where a difference of as high as 30% can also be seen. From the 1st to the 8th loading, a resistance reduction of 30% can be observed at low pressures.

4.5. Effect of hysteresis behavior

Heat management of PEMFCs is essential over the course of their operational lifetime. Starts-up and shuts-down of a PEMFC during
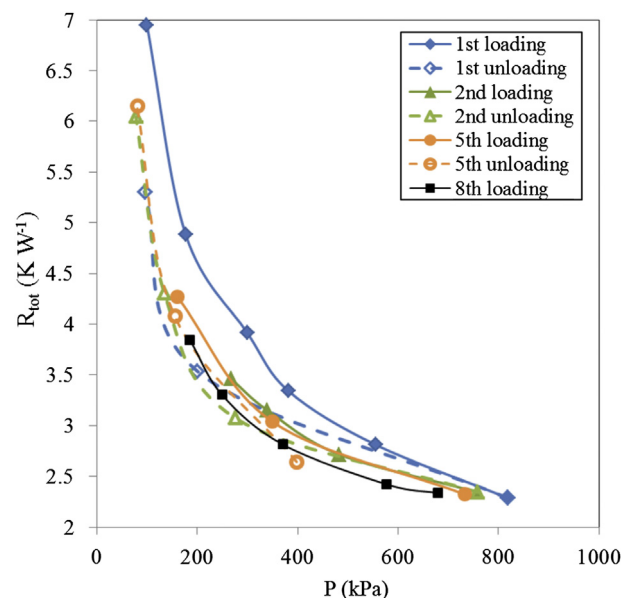

Fig. 11. Variation of GDL thickness with compression.

Fig. 12. Effect of different successive cyclic loads on the total resistance of SGL 34BC at the temperature of 60 °C.
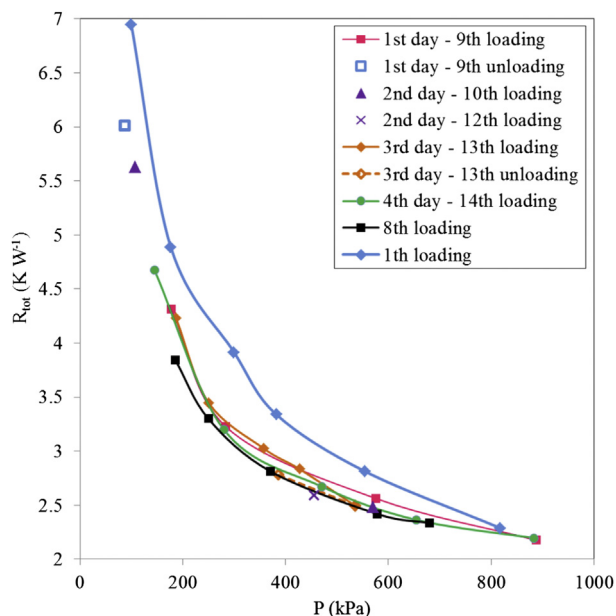
Fig. 13. Hysteresis behavior of subsequent discontinuous load cycles on the already-tested sample of SGL 34BC (related to Fig. 12) over 4 successive days.

its lifetime can cause discontinuous compressions and releases, here referred to as hysteresis effect, which is different from the cyclic compression effects. In fact, discontinuous successive compressions and releases performed at different periods of time are led to hysteresis behavior of fuel cell components.

Fig. 13 shows the hysteresis behavior of the already-tested sample of SGL 34BC for subsequent discontinuous cyclic compression tests conducted over 4 successive days. The data of the first and eighth loadings of sample 34BC, already shown on Fig. 12, are also added to Fig. 13 to facilitate comparison of the hysteresis behavior with the successive loading behavior and also with the behavior of a virgin sample. It is worthwhile noting that the sample resistances related to each of the 4 test days always lay within the resistances of the first and last (eighth) compressive loadings already exerted on the sample. In fact, discontinuous compressive tests performed over 4 separate days on the already-tested sample have never been led to resistances as high as the total resistance of the virgin sample (1st loading). It is evident from Fig. 13 that there is a big difference between the first loading and the subsequent ones, which shows the noticeable irreversible behavior of compressed GDLs in terms of thermal resistance.

5. Summary and conclusion

Thermal conductivity of 14 SGL GDLs and its thermal contact resistance with iron clamping surfaces was modeled and measured at the temperature of around 60 °C at a compression range of 2–14 bar. The carefully conducted measurements, using an equipped, advanced device and including accurate de-convolution between bulk and contact resistance, helped resolve some contradictory observation reported in the literature and provided new insights:

- Both PTFE and MPL reduce thermal conductivity (even though porosity decreases).
- Both PTFE and MPL increase the contact resistance of GDLs with iron surfaces.
- MPL increases the contact resistance dramatically compared to untreated GDLs or GDLs with low PTFE content.

- Thermal conductivity of MPL and its contact resistance with iron surface were accurately measured.

In addition to determining the thermal conductivity of GDLs coated with MPL, the experimental procedure presented allowed estimation of the thermal contact resistance between the MPL and the GDL. The results show that this contact resistance is not negligible, and together with the MPL bulk resistance, accounts for roughly half of the GDL total resistance.

In addition to the experimental measurements, a new analytical model was developed and shown to allow robust and accurate prediction of the thermal conductivity of GDLs treated with PTFE. The model faithfully captures the trend of the experimental data and takes into account all the salient geometrical parameters, compression, and PTFE distribution inside the GDL. This model should prove useful for implementation in fuel cell performance models as well as in design.

Appendix A

A1. Methodology: two-thickness method

The thermal resistance relation for a single homogeneous sample sandwiched between the two fluxmeters can be written as:

$$R_{tot} = \frac{t}{kA} + 2TCR \tag{A.1}$$

where t and k represent the thickness and the thermal conductivity of the sample, respectively; A stands for the cross-sectional area of each fluxmeter and of the sample, TCR shows the thermal contact resistance between the sample and the fluxmeters, and R_{tot} represents the total resistance, which is the only measurable one.

The term t/kA in Eq. (A.1) represents the sample thermal resistance (R) that changes with the thickness. The sample thermal
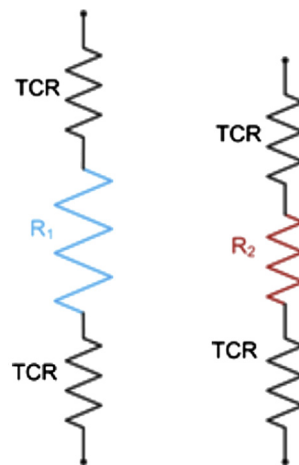

Fig. A.1. Thermal resistance network for samples with different thicknesses ($R_1 = t_1/kA$ and $R_2 = t_2/kA$).

conductivity k and the TCR are the two unknowns to be solved for. Therefore, another equation is needed in order to obtain the thermal conductivity. Assuming that the TCR depends on the interfacial characteristics but is independent of the sample thickness [36,37], a second equation can be provided using an identical sample but of a different thickness, so that no new unknown is added to the calculations, as illustrated in Fig. A.1.

The system of two equations containing the two unknowns, k and TCR, can be solved to obtain the thermal conductivity of the samples as:

$$k = \frac{(t_2 - t_1)}{(R_{tot1} - R_{tot2})A} \qquad (A.2)$$

where subscripts 1 and 2 represent the values for samples with different thicknesses of t_1 and t_2, respectively. The above method, referred to as the two-thickness method, is an accurate and effective way of de-convoluting the thermal contact resistance from the total resistance that is experimentally measurable.

A2. Principle of MPL thermal conductivity measurement

For MPL thermal conductivity measurements, the measured total resistance of the GDL ($R_{SGL\ BC}$) can be expanded as:

$$R_{SGL\ BC} = TCR_{MPL-FM} + R_{sub} + R_{MPL} + TCR_{sub-MPL} + TCR_{sub-FM} \qquad (A.3)$$

where TCR_{MPL-FM} is already available from measurements of the thermal bulk and contact resistances of GDL samples SGL 24 & 34BC themselves. The terms R_{sub} and TCR_{sub-FM} are respectively the resistance of the substrate, i.e., BA-type SGL samples of the same type (here 24BA or 34BA), and its contact resistance with fluxmeters, which have already been obtained from the measurements for GDLs SGL 24 & 34BA. The only two unknowns in Eq. (A.3), i.e., R_{MPL} and $TCR_{sub-MPL}$, can now be determined using Eq. (A.3) applied to two BC-type SGL GDLs (SGL 24 & 34BC). A similar procedure was performed on GDLs SGL 25 & 35BC. It should be noted that accounting for a thermal contact resistance between the substrate and MPL does not affect the MPL thermal conductivity calculation according to Eq. (A.2).

References

[1] EG&G Technical Services, Fuel Cell Handbook, Parsons, Inc., Morgantown, West Virginia, 2000.
[2] M.M. Mench, Fuel Cell Engines, John Wiley & Sons, 2008.
[3] A. Radhakrishnan, Thermal Conductivity Measurement of Gas Diffusion Layer Used in PEMFC. M.S. thesis, Rochester University, USA, 2009.
[4] D.L. Wood, R.L. Borup, in: Felix N. Büchi, Minoru Inaba, Thomas J. Schmidt (Eds.), Polymer Electrolyte Fuel Cell Durability, Springer, New York, 2009, pp. 159–195, http://dx.doi.org/10.1007/978-0-387-85536-3.
[5] N. Djilali, Energy 32 (2007) 269–280.
[6] K.J. Lange, P.C. Sui, N. Djilali, J. Power Sources 208 (2012) 354–365.
[7] B. Markicevic, N. Djilali, J. Power Sources 196 (5) (2011) 2725–2734.
[8] N.A. David, P.M. Wild, J. Hu, N. Djilali, J. Power Sources 192 (2009) 376–380.
[9] N. Djilali, D. Lu, Int. J. Therm. Sci. 41 (2002) 29–40.
[10] A. Tamayol, F. McGregor, M. Bahrami, J. Power Sources 204 (2012) 94–99.
[11] A. Tamayol, M. Bahrami, J. Power Sources 196 (2011) 6356–6361.
[12] N. Zamel, E. Litovsky, Xi. Li, J. Kleiman, Int. J. Hydrogen Energy 36 (2011) 12618–12625.
[13] N. Zamel, E. Litovsky, S. Shakhshir, Xi. Li, J. Kleima, Appl. Energy 88 (2011) 3042–3050.
[14] G. Karimi, X. Li, P. Teertstra, Electrochim. Acta 55 (2010) 1619–1625.
[15] M. Khandelwal, M.M. Mench, J. Power Sources 161 (2006) 1106–1115.
[16] O. Burheim, J.G. Pharoah, H. Lampert, J. Fuel Cell Sci. Technol. (2011), http://dx.doi.org/10.1115/1.4002403.
[17] O. Burheim, P.J.S. Vie, J.G. Pharoah, S. Kjelstrup, J. Power Sources 195 (2010) 249–256.
[18] J. Yablecki, A. Bazylak, J. Power Sources 217 (2012) 470–478.
[19] Z. Fishman, A. Bazylak, J. Electrochem. Soc. 158 (2011) B841–B845.
[20] H. Sadeghifar, M. Bahrami, N. Djilali, J. Power Sources (2013), http://dx.doi.org/10.1016/j.jpowsour.2013.01.086.
[21] E. Sadeghi, M. Bahrami, N. Djilali, J. Power Sources 179 (2008) 200–208.
[22] A. Pfrang, D. Veyret, G. Tsotridis, in: Amimul Ahsan (Ed.), Convection and Conduction Heat Transfer, InTech, 2011, ISBN 978-953-307-582-2.
[23] M. Bahrami, M.M. Yovanovich, J.R. Culham, J. Tribol. Trans. ASME 127 (2005) 884–889.
[24] SGL Group – The Carbon Company. SIGRACET Diffusion Media, Manufacture Data Sheet, 2013. Web: http://www.sglgroup.com/cms/international/home.
[25] G. Unsworth, N. Zamel, Xi. Li, Int. J. Hydrogen Energy 37 (2012) 5161–5169.
[26] J. David Sole, Investigation of Novel Gas Diffusion Media for Application in PEM Fuel Cell Ribbon Assemblies. M.S. thesis, Virginia Polytechnic Institute and State University, USA, 2005.
[27] M.M. Mench, E.C. Kumbur, T. Nejat Veziroglu (Eds.), Polymer Electrolyte Fuel Cell Degradation, Academic Press (Elsevier), MA, USA, 2012.
[28] N. Zamel, J. Becker, A. Wiegmann, J. Power Sources 207 (2012) 70–80.
[29] P. Teertstra, G. Karimi, X. Li, Electrochim. Acta 56 (2011) 1670–1675.
[30] S.F. Burlatsky, W. Atrazhev, M. Gummalla, D.A. Condit, F. Liu, J. Power Sources 190 (2009) 485–492.
[31] K. Kang, H. Ju, J. Power Sources 194 (2009) 763–773.
[32] ASTM C177 – 10, Standard Test Method for Steady-state Heat Flux Measurements and Thermal Transmission Properties by Means of the Guarded-hot-plate Apparatus, ASTM International, Conshohocken, PA, 2004.
[33] E. Sadeghi, N. Djilali, M. Bahrami, J. Power Sources 196 (2011) 246–254.
[34] E. Sadeghi, N. Djilali, M. Bahrami, J. Power Sources 195 (2010) 8104–8109.
[35] E. Sadeghi, N. Djilali, M. Bahrami, J. Power Sources 196 (2011) 3565–3571.
[36] M. Bahrami, J.R. Culham, M.M. Yovanovich, G.E. Schneider, J. Heat Transf. Trans. ASME 126 (2004) 896–905.
[37] M. Bahrami, J.R. Culham, M.M. Yovanovich, G.E. Schneider, J. Appl. Mech. Trans. ASME 59 (2006) 1–12.
[38] H. Sadeghifar, M. Bahrami, N. Djilali, in: ASME 11th Fuel Cell Science, Engineering and Technology Conference, July 14–19, 2013, Minneapolis, MN, USA, Paper No. ES-FuelCell2013-18070.
[39] H. Sadeghifar, M. Bahrami, N. Djilali, in: ASME 11th Fuel Cell Science, Engineering and Technology Conference, July 14–19, 2013, Minneapolis, MN, USA, Paper No. ES-FuelCell2013-18072.
[40] Iwao Nitta, Olli Himanen, Mikko Mikkola, Thermal Conductivity and Contact Resistance of Compressed Gas Diffusion Layer of PEM Fuel Cells, Fuel Cells 8 (2008) 111–119.
[41] M.K. Debe, Nature 486 (2012) 43–51.

Nomenclature

A: cross-sectional area of sample or fluxmeters, m^2
AA, BA, DA, BC: different types of SIGRACET GDLs (0, 5, 20, 5 (&MPL on side) % PTFE, respectively)
d: fiber diameter, m
GDL: gas diffusion layer, –
k: thermal conductivity
k_{eff}: effective thermal conductivity, W m^{-1} K^{-1}
k_{FM}: thermal conductivity of fluxmeter, W m^{-1} K^{-1}
l: distance between fibers in the x-direction, m
MPL: micro porous layer, –
P: compression pressure, bar or kPa
$PEMFC$: polymer electrolyte membrane fuel cell, –
$PTFE$: polytetrafluoroethylene
$PTFE'$: PTFE trapped between two fibers at their conjunction at the top block of the unit cell
$PTFE''$: PTFE trapped between two fibers at their conjunction at the top block of the unit cell
$PTFE'''$: PTFE extended along fibers
$PTFE_{layer}$: a thin layer of PTFE on the fibers of the first and last layers of GDL
Q: heat transfer through the fluxmeters, W
R: thermal resistance, K W^{-1}
SGL: SIGRACET
T: temperature, K
t: thickness, μm
TCR: thermal contact resistance, –
w: distance between fibers in the y-direction, m
$wt\%$: weight percent
x: position of thermocouples inside fluxmeters, m

Subscript
MPL: micro porous layer
eff: effective value
tot: total
sub: GDL substrate
GDL: gas diffusion layer, –
g: gas (see Refs. [20,21])
gc: gas filled gap (see Refs. [20,21])
1: related to thickness 1 or block 1 of unit cell (see Refs. [20,21])
2: related to thickness 2 or block 2 of unit cell (see Refs. [20,21])